



Sedimentological Influence on Physical Properties of a Tight Sandstone Reservoir: The Cretaceous Nenjiang Formation, Southern Songliao Basin, Northeast China

Jinkai Wang^{1,2*}, Jialin Fu¹, Jieming Wang³, Kai Zhao³, Jinliang Zhang⁴ and Jifu Liu⁴

¹College of Earth Science and Engineering, Shandong University of Science and Technology, Qingdao, China, ²Laboratory for Marine Mineral Resources, Qingdao National Laboratory for Marine Science and Technology, Qingdao, China, ³Research Institute of Petroleum Exploration and Development, Beijing, China, ⁴College of Resources Science and Technology, Beijing Normal University, Beijing, China

OPEN ACCESS

Edited by:

Jon Jincal Zhang,
Sinopec Tech Houston Center
(STHC), United States

Reviewed by:

Chao Liang,
China University of Petroleum
(Huadong), China
Deyong Li,
Ocean University of China, China
David Mark Hodgson,
University of Leeds, United Kingdom

*Correspondence:

Jinkai Wang
wangjk@sdust.edu.cn

Specialty section:

This article was submitted to
Sedimentology, Stratigraphy
and Diagenesis,
a section of the journal
Frontiers in Earth Science

Received: 15 September 2020

Accepted: 06 January 2021

Published: 24 February 2021

Citation:

Wang J, Fu J, Wang J, Zhao K,
Zhang J and Liu J (2021)
Sedimentological Influence on Physical
Properties of a Tight Sandstone
Reservoir: The Cretaceous Nenjiang
Formation, Southern Songliao Basin,
Northeast China.
Front. Earth Sci. 9:606701.
doi: 10.3389/feart.2021.606701

Abstract: The Nenjiang Formation, south of Songliao Basin, has many hydrocarbon bearing units, but currently the understanding of the distribution of viable reservoir sandstones is too limited to support a development strategy. Therefore, a detailed study on the sedimentary microfacies and reservoir properties has been completed in order to reduce uncertainty and improve subsurface predictions. Nine lithofacies and five lithofacies associations were identified supporting the development of a sedimentary model of a river-dominated delta front setting, which could be divided into four sedimentary environments: subaqueous distributary channel-fill, mouth bar, sand sheet, and interdistributary bay. The distribution sandbodies extend to the south in a tongue-like form, and they thin and pinch out. Finally, the influence of sedimentary process on properties was assessed by establishing the correlation between microfacies and reservoir physical parameters, such as porosity, permeability, pore radius, throat radius, and clay minerals. It is revealed that the correspondence between reservoir physical properties and microfacies types is strong; the physical properties of the subaqueous distributary channel and mouth bar are the best.

Keywords: southern Songliao basin, sedimentary characteristics, diagenesis, rock facies, lithofacies

INTRODUCTION

Lithofacies are identified by mineral composition, structure, color, and sedimentary structure of rocks, which is directly related to the sedimentary environment and facies of siliciclastic rocks. Early lithofacies type analysis and application were based on fluvial facies sandbodies (Miall, 1985). The changes of lithofacies characteristics reflect the changes of various conditions during the formation of sandbodies of different scales, such as hydrodynamic conditions, sediment transport mode, and the degree of external interference (Qi et al., 2009; Wu D. et al., 2019). The combination of these single lithofacies forms lithofacies associations, which is the result of multistage sedimentation and superposition (Eyles et al., 2010; Ding et al., 2014). Lithofacies associations and the arrangement of architectural elements can be used to interpret the climatic and environmental conditions during deposition and the paleohydrodynamic conditions (Jin et al., 2019).

According to the literature, many researchers have carried out conventional, but not detailed, sedimentary facies research in the Songliao Basin. These studies were usually at a large scale and the fourth member of the Cretaceous Nenjiang Formation was presumed to be a single prograding sequence (Liu et al., 1993; Sun et al., 2006). Most authors interpreted that tectonic movement controls the sedimentary facies types in the southern Songliao Basin (Li et al., 2009; Huang et al., 2013; Wang J. et al., 2014); the sedimentary facies types of the Nenjiang Formation in the Songliao Basin are gravity flows, alluvial fans, deltas, and rivers (Zhang et al., 2014; Li et al., 2015; Lv et al., 2016; Wang D.-d. et al., 2016). In this sedimentary period, there are two main river deltas, one comes from the northeast, which plays an important role in the sedimentary process of the first member of the Nenjiang Formation, the other comes from the east (Liu et al., 2016; Wang W. et al., 2016). Other interpret that the Nenjiang Formation in the Songliao Basin is a mud-prone delta with poor continuity, which has minor sand components and a lower angle, compared with the traditional delta. In addition to delta sedimentary environments, other sedimentary environments of the Nenjiang Formation include deep and shallow lakes (Gao and Wang, 2010; Wang L. et al., 2014) and even deep-water turbidite fans (Pan et al., 2017; Wang et al., 2018). Recently, some researchers established a new ultrafine-grained sedimentary model in the Songliao Basin: the channel fan, which includes straight and sinuous channels extending from north to south. This system is dominated by fine sediment and contains a large amount of sandstone, fluvial sedimentary structure, and internal erosion surfaces. In addition, the system also contains abundant terrestrial organic debris, showing bedload and suspended load transport (Tong et al., 2018; Mo et al., 2019). A series of diagenetic processes will occur after sediment deposition, which will directly affect the size and sorting of reservoir pores (Guo and Mao, 2019). Compaction and cementation greatly reduce the porosity of the reservoir, and at the same time the pore throats are blocked and the rock permeability is also greatly reduced, which is the main factor behind the formation of tight reservoir (Shi et al., 2015; Yang et al., 2017). However, in the middle and late diagenesis, some organic acid solutions will dissolve mineral particles and cements in pores, thus expanding the pores of rocks and improving its permeability. The main minerals of dissolution are potash feldspar and calcite (Wang et al., 2020). However, the location and degree of dissolution are quite different, which will lead to a different degree of dissolution of rock particles and cements, resulting in less strength in the correlation between porosity and permeability, and being prone to high porosity, low permeability, or high permeability and low porosity (Wang et al., 2018).

Many research results have made the structural evolution characteristics and sedimentary environment of Changling fault depression in the south of Songliao Basin clear, which provide a wealth of sources for this study (Meng et al., 2016; Xu et al., 2019; Cai et al., 2020). However, the characterization of sedimentary facies and evaluation of the fourth member of Nenjiang Formation in the south of Songliao Basin are not sufficient and need detailed research (Li et al., 2017; Zhang and Wang, 2019). Here, we refine the characterization of

microfacies in the areas with high well density to establish corresponding lithofacies models (either single or composite lithofacies model) and investigate the influence of sedimentation and diagenesis on reservoir physical properties. Through the study of fine reservoir description, we establish a new integrated sedimentary model and lithofacies model, discuss the factors controlling the sandstone physical properties, and play a positive guiding role in the effective development of this reservoir.

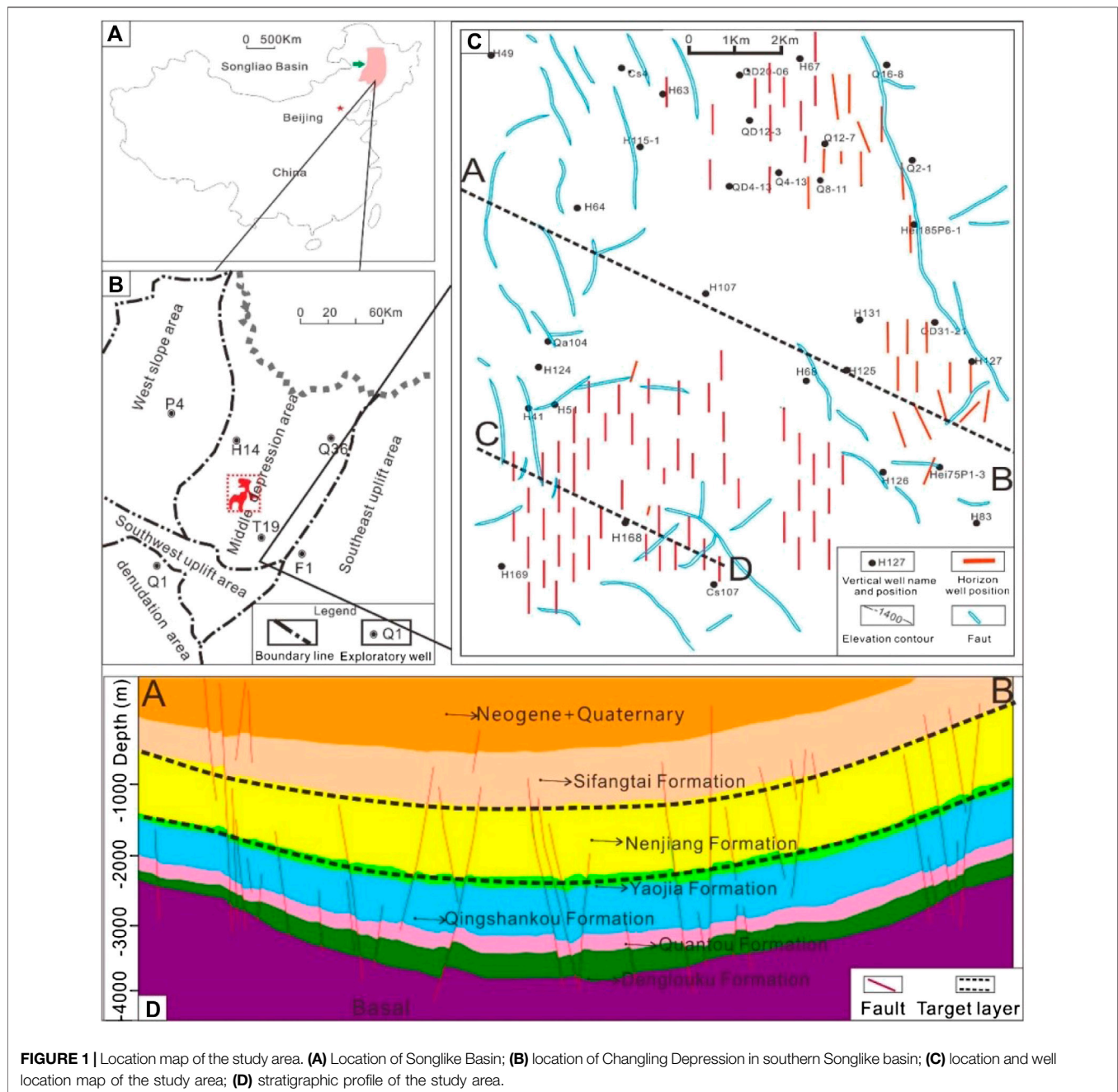
GEOLOGICAL SETTING

General Situation of the Study Area

Songliao Basin is the largest inland sedimentary basin fill of Mesozoic Cenozoic in eastern China, which is divided into two parts, the south and the north, with Songhua River as the boundary. The southern Songliao Basin comprises four first-order structural units: western slope, central depression, southeast uplift, and southwest uplift, among which the central depression and southeast uplift are important geological units for hydrocarbon exploration (Figures 1A,B) (Li et al., 2007; Zhang and Huang, 2010). The study area (H168 block) is located in Qian'an County, in Songyuan City of the Jilin province northeast of China, and its regional tectonic location is in the south of the Changling depression of the southern Songliao Basin. The structural characteristics of the Changling sag are relatively gentle. Its tectonic evolution has gone through three stages: early fault subsidence, middle subsidence, and tectonic quiescence. It mainly includes the Qian'an subsag and Heidimiao subsag, and the Hei168 block is located in the Heidimiao subsag, its east part is Huazijing terrace, and its northwest part is Daan-Honggang terrace. At present, 122 horizontal wells have been drilled and 117 wells have been put into production in the study area, which is a typical thin-layer reservoir developed by horizontal wells (Figures 1C,D).

Stratigraphic and Tectonic Evolution in the Study Area

Overall, the Songliao Basin experienced warm, humid climate during the Cretaceous period (Liu et al., 2003). The tectonic process includes three stages: early fault depression, middle depression, and late shrinkage. During the basin expansion stage (the early fault depression and middle depression stages), the Dengloulou Formation, Quantou Formation, Qingshankou Formation, and Yaojia Formation were successively deposited in the study area. In the low subsidence stage (the late shrinkage stage) of the basin evolution, deltaic and lacustrine strata are Nenjiang Formation (Figure 2A), Sifangtai Formation, and Mingshui Formation. The Yanshan V episode tectonic movement in the late Mingshui Formation resulted in strong inversion and uplift, forming the present structural form. The period of the Nenjiang Formation is the last stage (Li et al., 2018). The Nenjiang Formation comprises a large delta that built out into a lacustrine water body during the second flooding period



(Feng and Zhang, 2012; Huang et al., 2013). The relative lake level decreased continuously during the Nenjiang Formation period except for a short rise in the middle of the fourth member, and the main sedimentary types are semideep lake, delta, and shallow lake (Figure 2B).

METHODOLOGY

In this study, we obtained 35 rock samples of 4 cored wells (HN-20-1, HH75-X-4, QE37-14, and HF-5-2) at different depths.

Using these rock samples, a large number of micro characterization experiments have been carried out by means of optical or electronic microscope, such as thin section analysis, scanning electron microscope, and X-ray diffraction analysis experiment. On the basis of these experimental results, the micro components, pore structure, and diagenesis of reservoir sandstone have been characterized in detail, and the single and combined lithofacies models are established. Then, the characteristics of rock lithology, sandstone type, grain size, and sorting are studied in detail, the plan form and vertical distribution of microfacies are characterized, and the

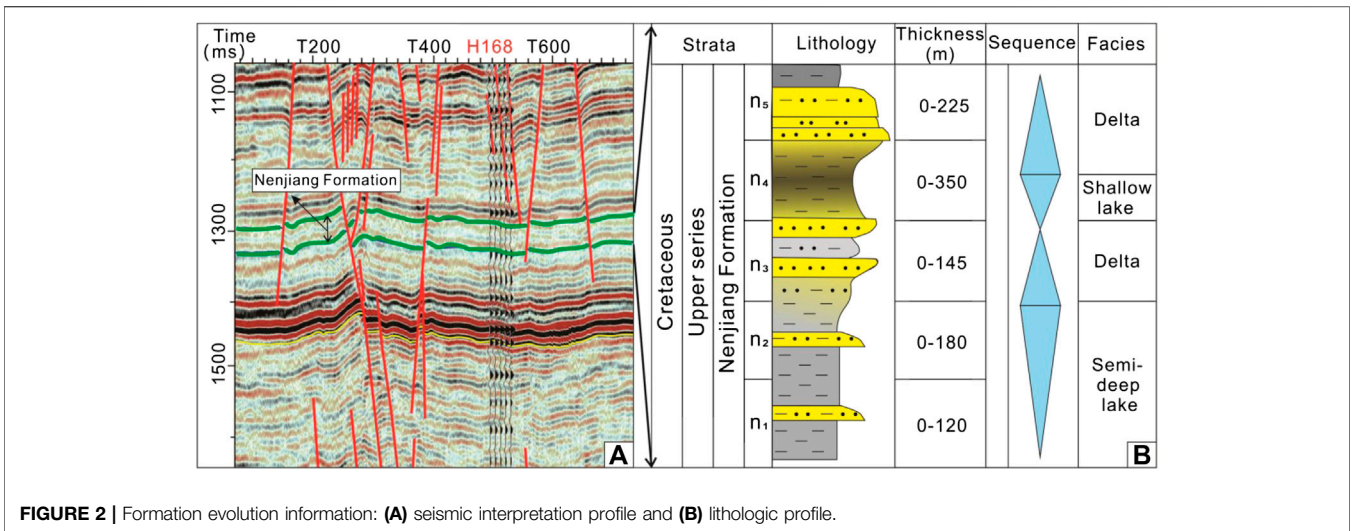


FIGURE 2 | Formation evolution information: (A) seismic interpretation profile and (B) lithologic profile.

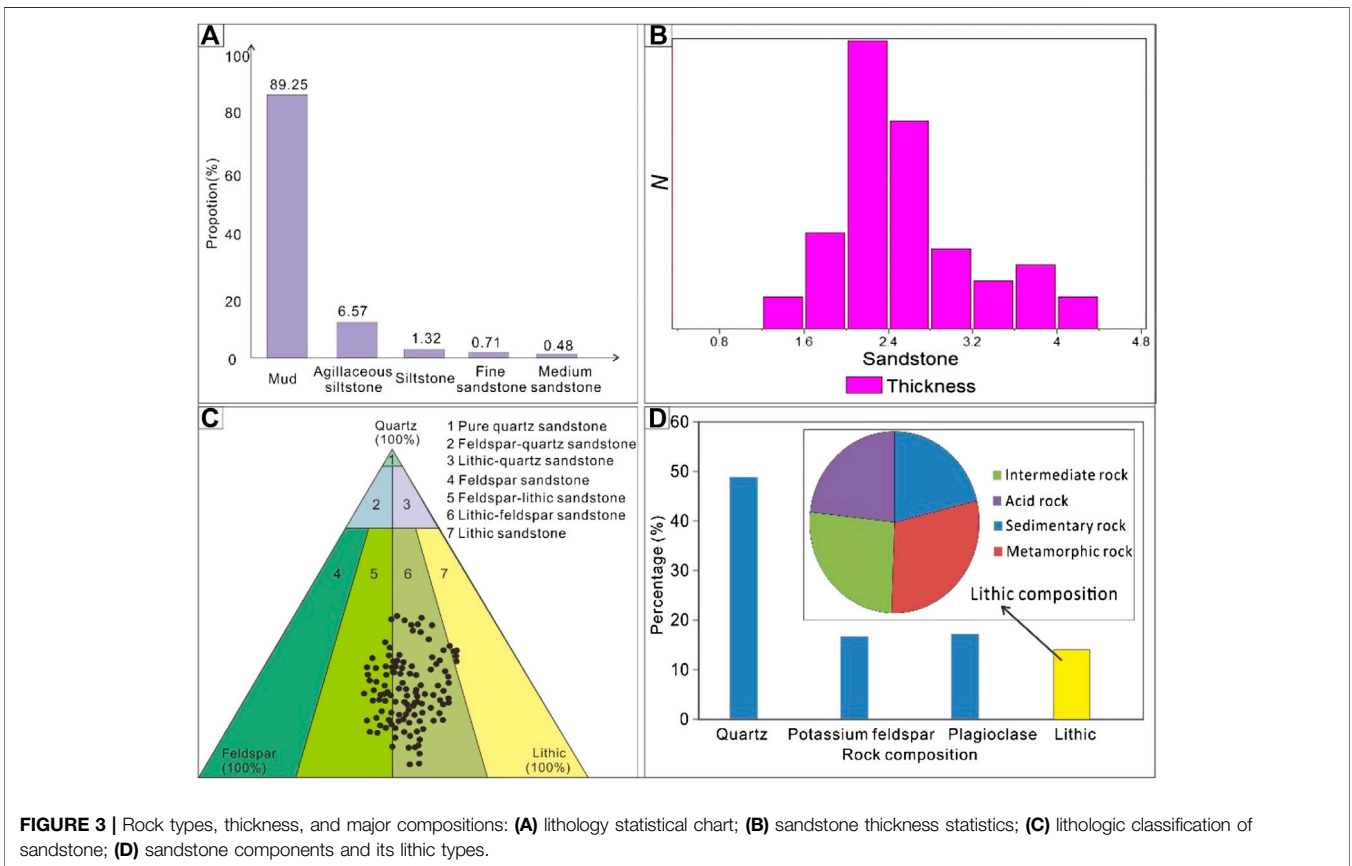


FIGURE 3 | Rock types, thickness, and major compositions: (A) lithology statistical chart; (B) sandstone thickness statistics; (C) lithologic classification of sandstone; (D) sandstone components and its lithic types.

sedimentary model is established. Finally, the sandstone diagenesis in the study area is characterized by using the micro pore structure experimental parameters, and the variation law of reservoir pore and throat, as well as their internal filler type, is clarified.

SEDIMENTARY CHARACTERISTICS

Lithologic Characteristics

The lithology of the fourth member of the Nenjiang Formation is mainly mudstone, whose content is as high as 90% (Figure 3A).

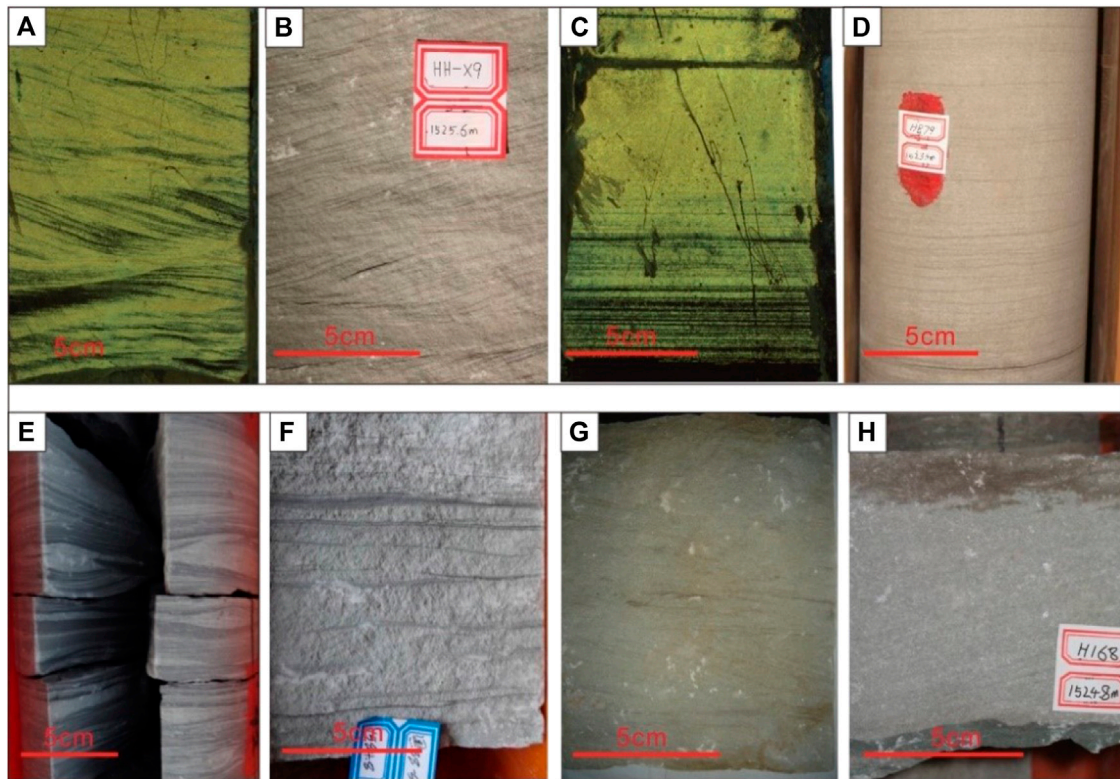


FIGURE 4 | Sedimentary structure of the study area: **(A)** HH75-X-4, 1446.5m, ripple cross lamination; **(B)** HH-9X, 1525.6m, ripple cross lamination; **(C)** HH75-X-4, 1456.8m, parallel bedding; **(D)** HH79, 1523.5m, parallel bedding; **(E)** HH-X9, 1520.4m, wavy bedding; **(F)** HE-88-2, 1584.8m, flaser bedding; **(G)** QE37-14, 1505.3m, trough cross bedding; **(H)** H168, 1524.8m, cross bedding.

The lithology of sandstone is mainly gray medium- and fine-grained sandstone, siltstone, and argillaceous siltstone, showing normal and inverse grading. The thickness range of a single sand body is 1–5 m, with an average of 2.2 m (**Figure 3B**). According to Folk's three terminal sandstone classification method (Folk, 1968), the relative content of quartz, feldspar, and rock debris shows that the main types of sandstone are lithic feldspar sandstone (**Figure 3C**), of which the average content of quartz is 32%; feldspar content is 31% (potash feldspar), and lithics is 37%, which includes igneous rocks, metamorphic rocks, and mica debris. All these suggest that the sediment source area is far away from the provenance area and belongs to the terminal position of the river (Wu J. et al., 2019), and the source area lithology is complex, mainly metamorphic rock and intermediate magmatic rock (**Figure 3D**).

Sedimentary Structure

Through core observation, it can be found that the sedimentary structures shown in the rocks in the study area mainly include cross bedding, parallel bedding, wavy bedding, and sand ripple bedding, which are consistent with an interpretation of the sedimentary environment of river-dominated delta front (**Figure 4**).

The sedimentary structures show weak hydrodynamic characteristics. The strong scour structures at the bottom of

the subaqueous distributary channel are rare; therefore, the trough cross bedding in the core is not obvious. The main sedimentary structure includes planer cross bedding, parallel bedding, ripple lamination, and other sedimentary structures. The single sand body of the mouth bar is relatively thick, mainly composed of fine sand and silty sand; the sedimentary structures include current sand ripple bedding, parallel bedding, low angle cross bedding, and wave formed sand ripple bedding. The sand sheet is well sorted and is mostly fine sandstone and siltstone. There is no large-scale cross bedding. Parallel bedding and low angle cross bedding are mainly developed. There are also sand ripple bedding and wavy bedding. The biogenetic structure is not developed.

The grain size parameters of sandstone in the study area were obtained by using the casting slice observation method. The grain size of the reservoir rock in the study area is generally small, and the cumulative curve of grain size probability is mostly two-stage (composed of jump population and suspension population). The particle size of the sediment is small, but the distribution range is large. The cut-off point between the saltating population and the suspended population is between 2.5Φ and 4.0Φ . The suspended population content is mostly between 10 and 40%, and the jumping population content is generally more than 60% (**Figures 5A–C**). In the C-M diagram, the sample points are concentrated in the QR segment and a few in the RS segment. The QR segment is parallel to the baseline of $C = M$, which represents

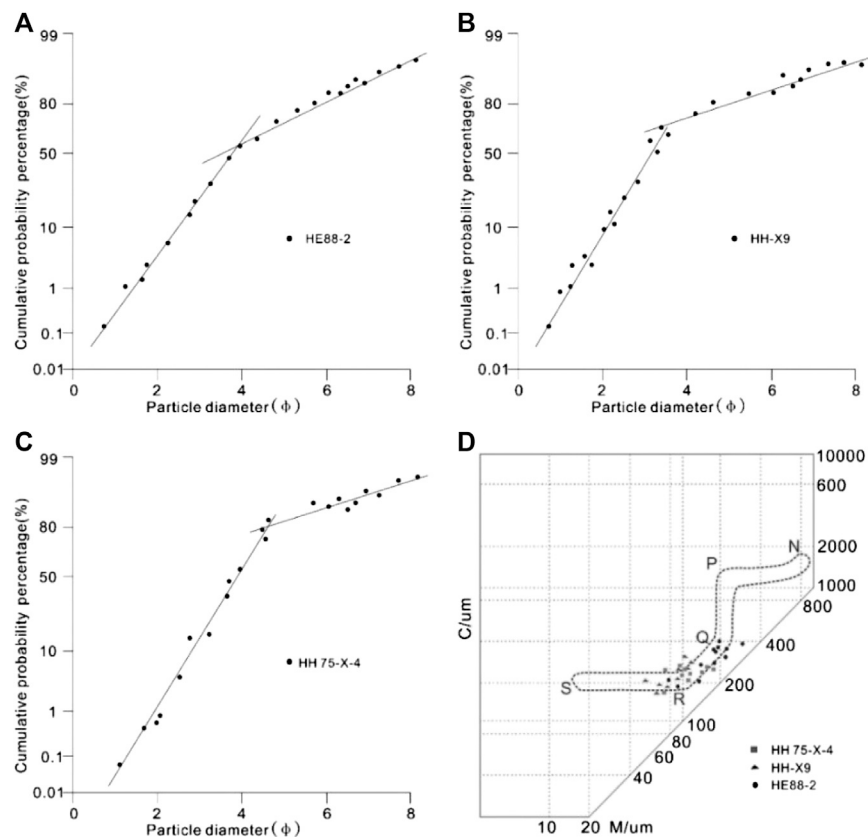


FIGURE 5 | Grain size cumulative probability curve and C-M diagram of sandstone: **(A–C)** cumulative curve of grain size probability and **(D)** the C-M diagram of different samples of three core wells.

the deposition mechanism of gradual suspension. In the fluid, the particle size of suspended materials gradually becomes finer from the base to the top, which is often caused by the development of turbulence, and its C and M increase in proportion. RS section is a uniform suspension, which is a complete suspension with no change of particle size and density with depth, reflecting a weak and calm sedimentary environment (Figures 5D).

Lithofacies Characteristics

The grain size range of sediments is relatively small, the types of sedimentary rocks are relatively unified, and the sedimentary sequences formed are relatively similar. It is difficult to distinguish their microfacies types from rock types alone and to understand the relationship between different microfacies types. Therefore, this study identifies sedimentary microfacies based on the combination of lithofacies characteristics. On the basis of identified lithofacies types, a model of single lithofacies and composite lithofacies is established.

(1) Single Lithofacies

Nine lithofacies types were identified in the delta facies according to the characteristics of rock fabric, bedding, and grain order of the study area (Cheng et al., 2017; Kallepalli

and Richardson, 2017); the morphology and characteristics of each lithofacies are shown in Figure 6.

These lithofacies include (1) the massive fine sandstone facies (FIM), which was formed under rapid deposition; (2) trough cross bedding sandstone facies (FIT), which was formed by migration of 3D dune-scale bedforms at the base of subaqueous distributary channel; (3) oblique bedding fine sandstone facies (FIO), which was usually formed in the deposition environment of mouth bar or sand sheet; (4) low-angle cross-bedding fine sandstone facies (FIL), which was usually formed by deposition in subaqueous distributary channels with weak current action; (5) inverse graded sandstone facies (SI), which was usually formed by waxing hyperpycnal flows that deposit on the mouth bar; (6) ripple cross lamination fine sandstone facies (PR), which was formed in a relatively quiet water environment and mainly composed of argillaceous siltstone; (7) ripple cross lamination and lenticular bedding siltstone facies (SiC), which was usually formed by the interdistributary bay setting; (8) ripple cross lamination siltstone facies (SiR), which was formed in the front of the river controlled delta with weak hydrodynamic force (Gugliotta et al., 2015; Xu et al., 2020); and (9) the horizontal bedding mudstone facies (MH), which was formed by suspension deposition in the interdistributary bay-fill.

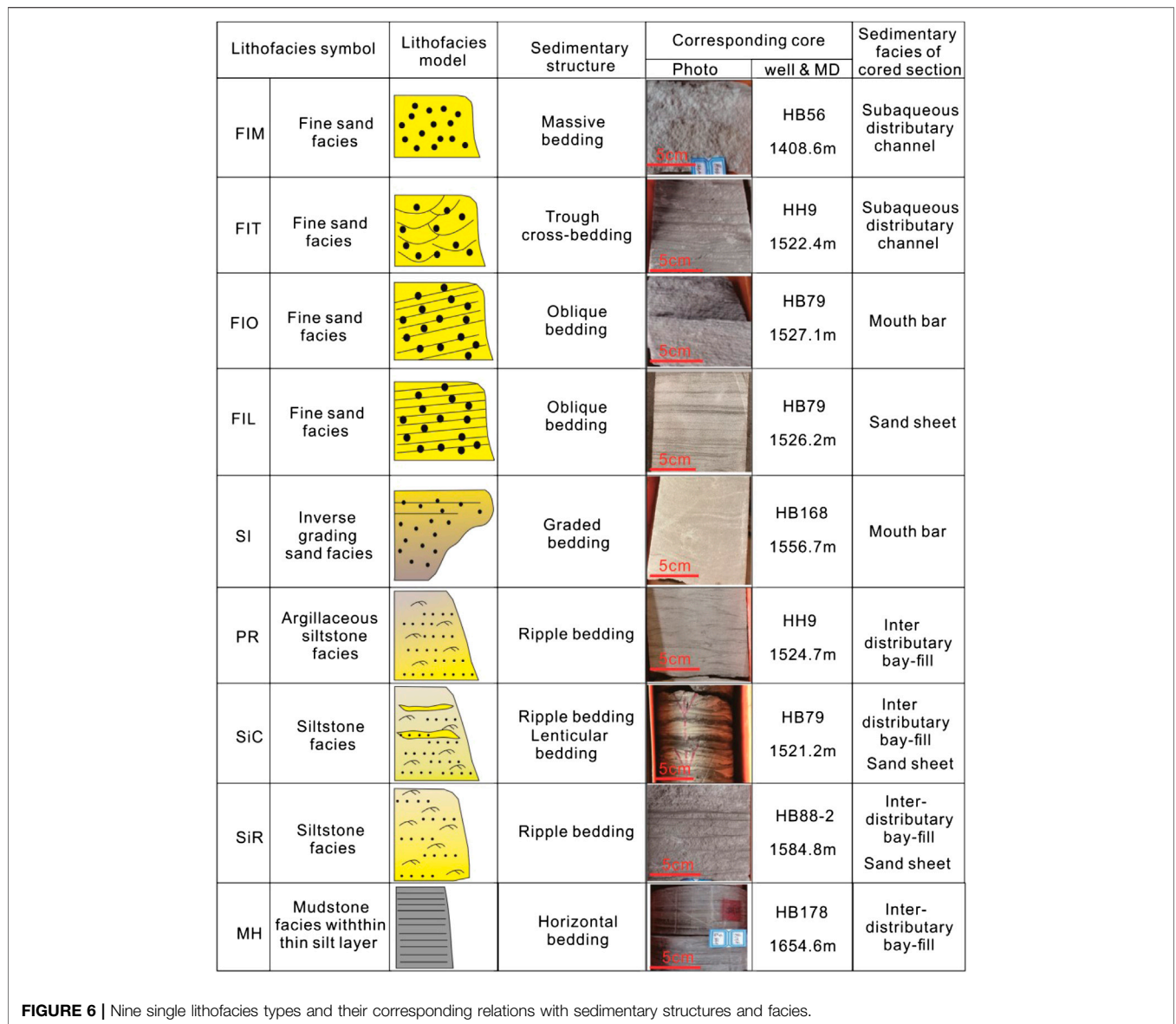


FIGURE 6 | Nine single lithofacies types and their corresponding relations with sedimentary structures and facies.

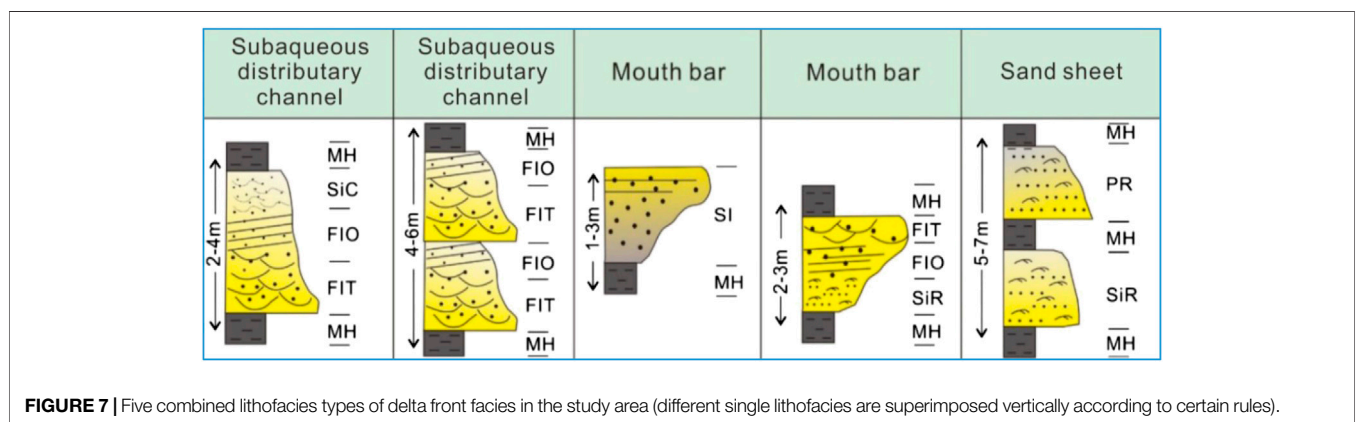


FIGURE 7 | Five combined lithofacies types of delta front facies in the study area (different single lithofacies are superimposed vertically according to certain rules).

TABLE 1 | Corresponding relationship between sedimentary microfacies and logging curves.

Microfacies types	Logging response characteristics	Logging curve shape SP GR	Well name	Sand body shape	Lithologic characteristics
Subaqueous distributary channel	Smooth box or bell-shaped characteristics	fx1	Hb178	Fx10	Fine sandstone equal grain size good properties
	Dentate box or bell-shaped characteristics	fx2	QD20-06	fx11	Fine sandstone muddy strips in the middle
Mouth bar	Low amplitude bell-shaped characteristics	fx3	Q4-13	fx12	Siltstone with higher clay content
	Smooth funnel-shaped characteristics	fx4	H115-1	fx13	Fine sandstone and siltstone good properties
	Medium or small funnel-shaped characteristics	fx5	QD31-21	fx14	Siltstone and argillaceous siltstone
Sand sheet	Medium or big finger-shaped characteristics	fx6	H83	fx15	Siltstone thin sand body
	Medium finger-shaped characteristics	fx7	H64	fx16	Siltstone and argillaceous siltstone thin sand body
Interdistributary bay-fill	Small finger-shaped characteristics	fx8	Q16-8	fx17	Argillaceous siltstone and silty mudstone
	Unobvious low-amplitude protrusion	fx9	HH79-8	fx18	Silty mudstone

(2) Lithofacies Combinations

Lithofacies were combined to form five lithofacies association identified according to observation and description of core. These are (1) MH-SiC-TIO-FIT-MH; (2) MH-FIO-FIT-FIO-FIT-MH; (3) SI-MH; (4) MH-FIT-FIO-SiC-MH; and (5) MH-PR-MH-SiC-MH. These lithofacies combination types coincide with sedimentary environments (**Figure 7**). The MH-SiC-TIO-FIT-MH type represents the single distributary channel deposition model, the MH-FIO-FIT-FIO-FIT-MH type is the main combination of lithofacies which is usually related to the vertical superposition of multiple channels, the SI-MH type and the MH-FIT-FIO-SiC-MH type are interpreted to represent mouth bar, and the MH-PR-MH-SiR-MH is related to splay in interdistributary bay-fills.

Sedimentary Facies and Microfacies Characteristics

Based on the analysis of lithological characteristics, sedimentary structure, and other sedimentary facies markers, combined with the sedimentary background and environment of the fourth member of the Nenjiang Formation of the Songliao Basin, the types of sedimentary facies are determined as a transgressive delta. By analyzing the lithology, rock color, lithofacies type, and other facies indicators, it can be concluded that the study area is located in the delta front. The delta front can be divided into four different parts in the study area: subaqueous distributary channel-fill, mouth bar, sand sheet, and interdistributary bay-fill. The log response characteristics, curve shape, sand body shape, and lithology of each sedimentary microfacies sand body are very different, which are their main distinguishing features (**Table 1**).

(1) Subaqueous Distributary Channel-Fill

The distributary channel is the subaqueous extension part of the onshore branch channel. In the process of extension, the channel widens, and the bifurcation increases, the flow velocity decreases, and the deposition rate increases. The lithology is

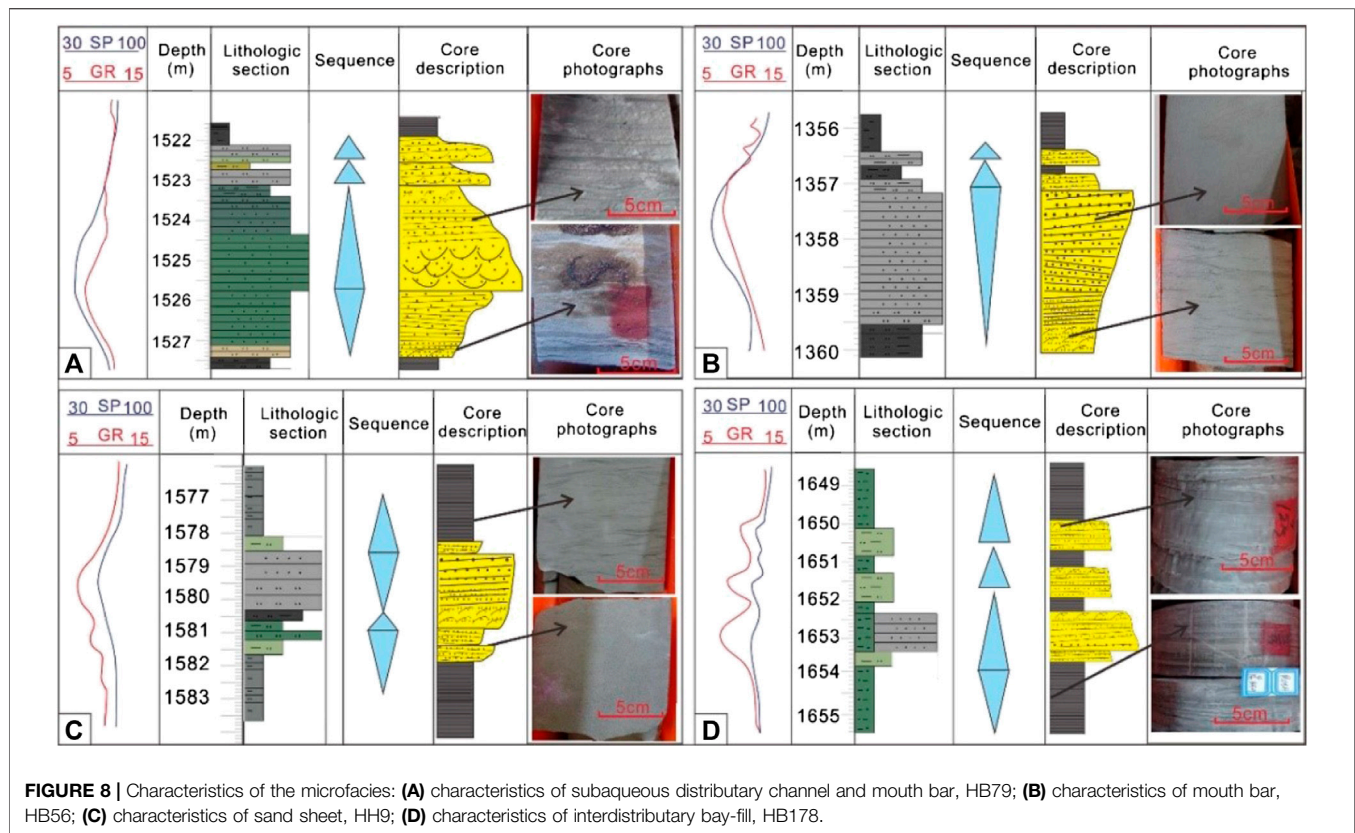
mainly grayish white fine to medium sandstone, with trough cross bedding, parallel bedding, and small trough cross bedding which can be seen from the bottom to the top; SP log curve is box shaped; sand body vertically presents a positive rhythm of coarse and fine from the bottom to the top. The subaqueous distributary channel-fill thickness in the study area is generally 2–4 m. The base of these sand bodies is an erosional overlain by trough cross bedding and muddy gravel. The middle is oblique bedded sandstone and the upper is laminated sandstone. The top is sand ripple bedding with an increased mud content (**Figure 8A**).

(2) Mouth Bar

The mouth bar formed after the branch channel entered the lake where the distributive channel bifurcates. Most of the mouth bar in the study area coarsens upward, increasing sand content and better sorting. SP log curve of the mouth bar sand body is funnel-shaped with abrupt change at the top and gradual change at the base. The mouth bar of the study area is mainly composed of fine sand and silty sandstone; its thickness is generally more than 2.5 m. The base of the sand body has more gradual contact with the underlying rock layer and the top contact is abrupt with the overlying mudstone layer. The bedding structures include small cross bedding, parallel bedding, and low angle oblique bedding (**Figure 8B**).

(3) Sand Sheet

The sand sheet is distributed in the front and flank of the mouth bar. It is characterized by a wide distribution area, but the particle size becomes smaller and the sandbodies become thinner. It is mostly distributed in the front of the delta front, where the hydrodynamic conditions are weak. The shape of SP log curve is usually finger- and cone-like, and the amplitude is generally high and medium. The sand sheet sandstone is well sorted; its lithology is mostly argillaceous siltstone and siltstone, with a thickness of 1–2 m. Small cross bedding, parallel bedding, and flow sand ripple bedding are usually found in the sand sheet, in addition to some biogenic structures (**Figure 8C**).



(4) Interdistributary Bay-Fill

Because of the river overflow and the change of water depth, an interdistributary bay forms. Longitudinally, it is usually composed of multiple sand bodies. There are mudstone interbeds in the middle of the sand bodies, and the thickness is uneven. In terms of internal structure, there are obvious interbeds between each single sand body and other sand bodies in the sequence. Log curves are similar through the sand bodies but have correlated peaks, which are generally tooth-shaped, conical, or elliptical, with moderate or low amplitudes, at the mudstone interbeds (**Figure 8D**).

DISCUSSION

Distribution of Sedimentary Microfacies

According to the distribution law of sedimentary microfacies, the Sanzhao and Gulong depressions in the northern part of the study area are the main source areas. The progradational delta distributed sediment southward along the long axis of the basin. The delta front facies sand bodies extend to the inner part of the study area, forming a reservoir mainly composed of sheet sand. The catchment area of Songliao Basin is in the south, basinward of the delta front subfacies, and the sedimentary microfacies are dominated by the sand sheet. Most of the thin layers in the fourth member of Nenjiang Formation are poor in physical properties, and there is no effective oil-bearing layer

(**Figure 9B**). The $k_2n_4^6$ sandbody thickness is 3–5 m, and the two microfacies, distributary channel-fill and mouth bar, account for a relatively high proportion. Therefore, its sand body has good physical properties, which is the main oil-bearing layer in the fourth member of Nenjiang Formation and the target member of our study (**Figure 9C**).

Analysis of previous research results shows that the sediments of the study area are derived from the northeast (Jia et al., 2007; Huang et al., 2013; Bao and Niu 2017). Affected by this, the thickness of sandstone in the northeast is larger than that in the southwest. The thickness of sand body decreases gradually from southwest to northeast until it pinches out. However, there is no boundary of sandstone disappearance in the study area. The distribution area of sandstone here is very large, and its thickness is between 1 and 4 m, with an average thickness of 3.5 m.

Sedimentary Model

According to the structural evolution characteristics of Songliao Basin and the sedimentary facies, a sedimentary model of river delta in the study area is established (**Figure 10**).

The sedimentary model is derived from the interrelationship between the sedimentary environment, sedimentation, and the results (sedimentary facies). The sedimentary model not only shows the most typical characteristics of sedimentary facies, but also shows the formation mechanism and process of sedimentary facies (Ye, 2005; Feng and Zhang, 2012; Gao et al., 2017). The sedimentary system of Songliao Basin was dominated by a process of progradation; during the first member and the

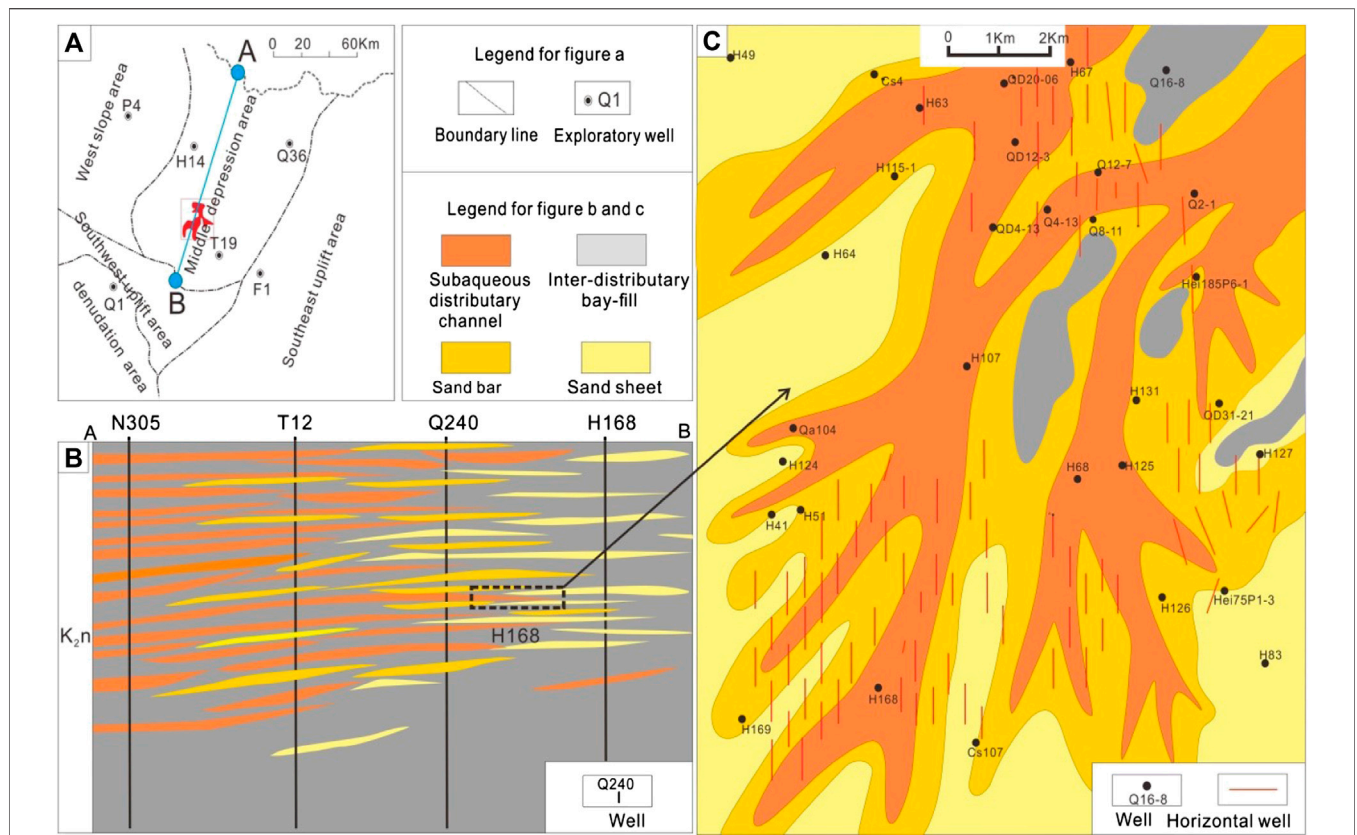


FIGURE 9 | Distribution map of sedimentary microfacies of the layer K2n46: **(A)** location of the southern Songlike Basin; **(B)** lithological profile of connecting wells, planar graph of the sedimentary microfacies.

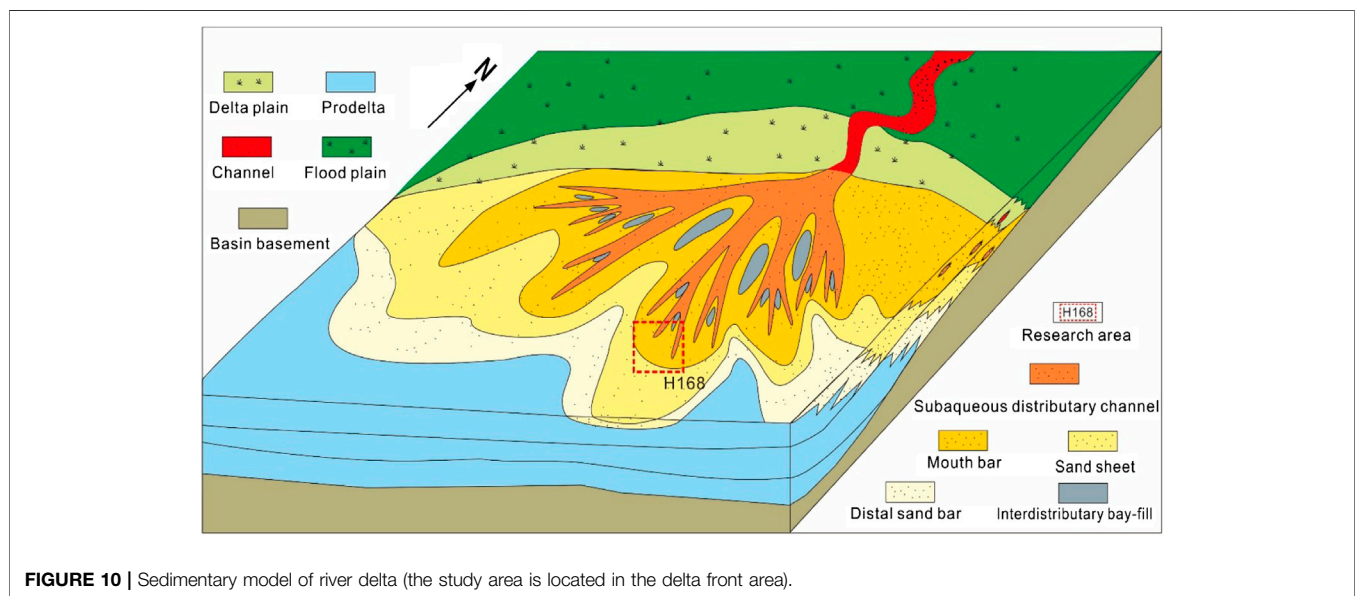


FIGURE 10 | Sedimentary model of river delta (the study area is located in the delta front area).

second member of Nenjiang Formation, the relative lake level rose and the water body deepened continuously. From the late stage of the second member of the Nenjiang Formation, the

relative lake level began to decrease until the third member ended. In the early stage of the fourth member of Nenjiang Formation, the basement tectonic activity in the southern Songliao Basin

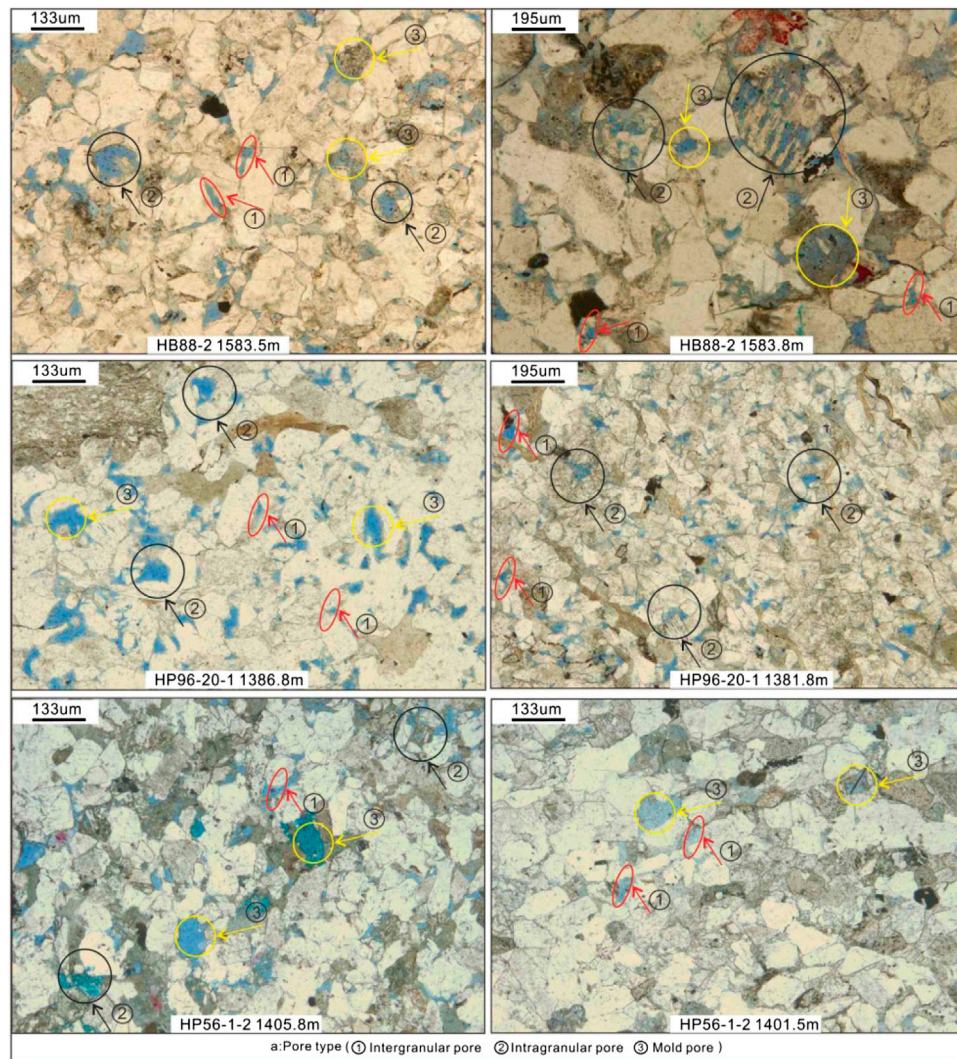


FIGURE 11 | The different pore types of the sandstone (① intergranular pores; ② dissolution pore of feldspar; and ③ mold pore of the debris dissolution).

gradually weakened, which entered the active period of depression. At the end of the fourth member of Nenjiang Formation, the relative lake-level fallen and the delta continued to prograde southward, forming the deposition dominated by mouth bar and sand sheet. The fifth member of Nenjiang Formation is a period of continuous rising of relative lake level.

Analysis of the Influence Degree of Sedimentation on Reservoir Properties

(1) Because the target area is located at the end of the delta front, distal to the source area, the deposits are predominantly fine-grained, and mudstone accounts for a relatively high proportion, sandstone are very fine grained, and the deposits are well sorted. Under the influence of these conditions, the pores of sandstone are relatively small, and the smaller intergranular pores are dominant (46%). In

addition, due to the influence of parent rock lithology in the source area, the content of feldspar and lithics in sandstone is higher, which increases the probability of particle dissolution. Therefore, the content of dissolution pores and mold pores related to dissolution is 29 and 17% respectively. Dissolution depends largely on the cement in the pores, and the content of early carbonate cement in the pores of the rock is very high, with an average of 18%, which is easily dissolved by the organic acid. But the clay mineral content is low (15%) mainly composed of illite/montmorillonite (I/M) mixed layer, which has little effect on the physical properties of the reservoir and only plays a role of interstitial filling, respectively. In addition, other types of pores in the rock are relatively small (Figure 11).

The probability distribution of sandstone pore and throat radius is obtained by using the constant velocity mercury injection experiment. The correlation between these data and

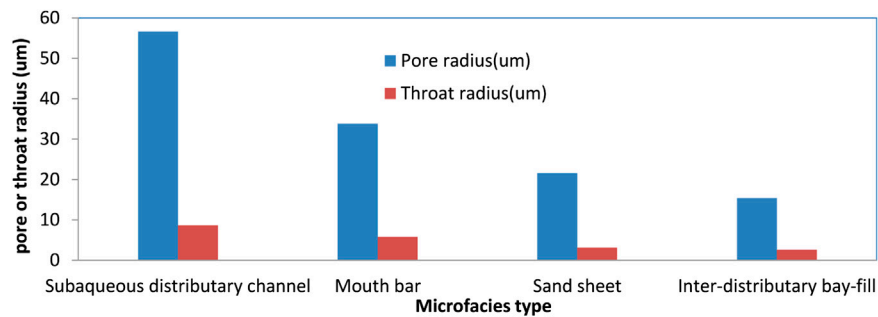


FIGURE 12 | Statistical chart of relationship between sandstone pore and throat size and microfacies.

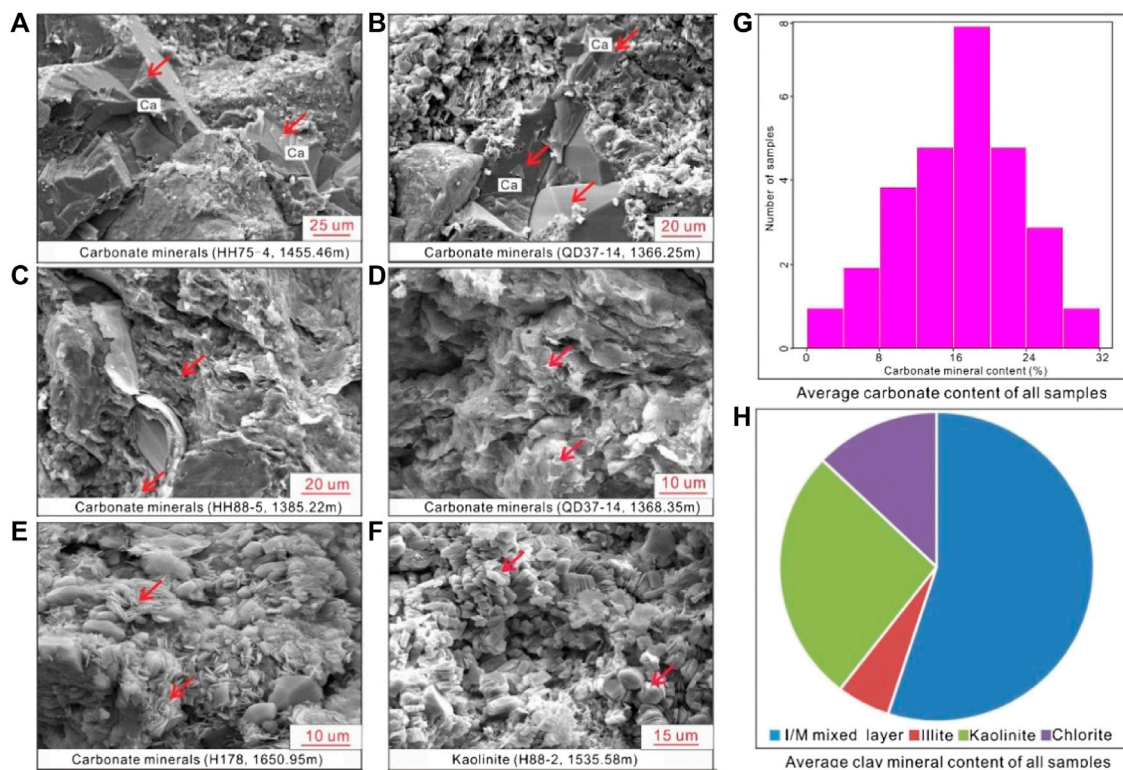


FIGURE 13 | Pore characteristics of sandstone: (A–F) pore structure and mineral characteristics observed by SEM; (G, H) content of different cementation minerals.

sedimentary microfacies shows that the physical conditions of distributary channel sandbodies are the best, which have good storage and seepage performance. The average of pore radius is 56.6 μm , and the average of throat radius is 8.6 μm . The physical conditions of the mouth bar sandbodies are the second, the average of pore radius is 33.8 μm , and the throat radius is 5.7 μm . The physical properties of the sand sheet body at the delta front are very poor, with an average pore radius of 21.5 μm and an average throat radius of 3.1 μm . The physical properties of the interdistributary sandbodies are the worst, with an average pore radius of 15.3 μm and an average throat radius of 2.5 μm , almost without storage and seepage performance. This shows that

the size and distribution of pores and throats are greatly influenced by sedimentary microfacies (Figure 12).

(2) Due to the influence of sedimentary environment, the sandstone in the study area has finer grain size, more argillaceous sediments, and high clay mineral content. The sandstone interstitial material includes mud, carbonate, and clay minerals; the mud is mostly recrystallized and locally distributed in a muddy strip (Zhang et al., 2018; Li et al., 2019; Zhang et al., 2020). Carbonate cementation (calcite and dolomite) is an important cementation, which is one of the main factors to destroy the reservoir conditions in the study

area. According to the precipitation sequence and composition changes, they can be divided into early and late stages.

The carbonate minerals in the study area are mainly early cements, which are mainly formed in the late stage of early diagenesis. The crystal morphology of calcite is generally poor, while that of dolomite is better (Figures 13A,B). The results of whole rock X-ray diffraction show that the mineral content of carbonate rock is between 5 and 25%, with an average of 18% (Figure 13G). The early carbonate cement fills the primary pores, reduces the porosity and permeability of rocks, and destroys the reservoir performance. The clay mineral content in the fourth member of Nenjiang Formation is relatively high, and clay cementation is also the most important cementation in the study area. Clay cements include the I/M mixed layer (Figure 13C), illite (Figure 13D), chlorite (Figure 13E), and kaolinite (Figure 13F) of which the content of the I/M mixed layer is the highest, reaching 55% (Figure 13H). This shows that the hydrodynamic conditions are weak, but later diagenesis is strong.

(3) Different microfacies lead to different types of sandbodies, which leads to great differences in porosity and permeability of rocks, so the distribution range of sandstone porosity and permeability of each microfacies can directly reflect the matching relationship between different sedimentary microfacies and reservoir physical properties. For the reservoir in the study area, the physical properties of the subaqueous distributary channel-fill and mouth bar are the best, with an average porosity of more than 13% and a permeability of more than $17 \times 10^{-3} \mu\text{m}^2$; the sand body of the sand sheet is the second, with a porosity of 10.48% and a permeability of $9.36 \times 10^{-3} \mu\text{m}^2$; the sandstone physical properties of the interdistributary bay-fill are the worst, with an average porosity of only 8.33% and a permeability of only $3.55 \times 10^{-3} \mu\text{m}^2$. The correspondence between the physical properties of the reservoir and the types of sedimentary microfacies is very good, which reflects the control of the depositional processes and detrital mineralogy on the reservoir performance, as have been interpreted from deep-water settings (Porten et al., 2016).

CONCLUSION

(1) The sandstone content of the K_2n_4 strata in southern Songliao Basin is merely 10%, which indicates long transport distance for the sediments. The sedimentary facies support interpretation of a river-dominated delta front which includes four microfacies: subaqueous distributary channel, mouth bar, sand sheet, and interdistributary bay-fill. The lake basin in the study area was gradually shrinking during the deposition period of Nenjiang Formation, and the river delta continued to prograde southward, which causes the sand body to become tongue-like and gradually thinned to the south.

(2) There are 9 single lithofacies types and five lithofacies associations in the target layer of the study area. The single lithofacies mainly consist of SIT, SR and PR, and the main combination of lithofacies is MH-FIT-FIO-FIT-FIO-MH, which show the vertical superposition of positive rhythm channel sand bodies. This is consistent with the characteristics of microfacies in the study area.

(3) Influenced by sedimentary environment and distance from source area, the grain size of sediment is very fine, which determines that the primary porosity and permeability of sandstone are low. In addition, the compaction and cementation in the diagenesis stage are strong, which reduces reservoir pore space. Therefore, the pores of the sandstone are mainly formed by lithic and feldspar dissolution in the study area. Dissolution depends largely on the cement in the pores, and the content of early carbonate cement in the pores of the rock is very high, with an average of 18%, but the clay mineral content of is low (15%) which is mainly composed of illite/montmorillonite- (I/M-) mixed layer. The absolute content of clay mineral has little effect on the physical properties of the reservoir and only plays a role of interstitial filling.

DATA AVAILABILITY STATEMENT

The original contributions presented in the study are included in the article/Supplementary Material; further inquiries can be directed to the corresponding author.

AUTHOR CONTRIBUTIONS

JW was mainly responsible for the conception of the article. He put forward a good idea and completed the research content related to sedimentary facies in the article. KZ was in charge of sedimentary facies research and carried out rock analysis experiments. JZ gave some good ideas to the lithofacies model establishing. Xie has been engaged in the research on the reservoir property influence factors.

FUNDING

Projects ZR2020MD035 was supported by the Natural Science Foundation of Shandong Province. Projects 51504143 and 51674156 were supported by the National Natural Science Foundation of China.

ACKNOWLEDGMENTS

The authors would like to thank workers from the Jilin oilfield for supplying the research data.

REFERENCES

- Bao, Y., and Niu, F. (2017). Constraining sedimentary structure using frequency - dependent p wave particle motion: a case study of the Songlike Basin in NE China. *J. Geophys. Res. Solid Earth* 122 (11), 9083–9094. doi:10.1002/2017JB014721
- Cai, J., Xu, K., Zhu, Y., Hu, F., and Li, L. (2020). Prediction and analysis of net ecosystem carbon exchange based on gradient boosting regression and random forest. *Appl. Energy* 262, 114566. doi:10.1016/j.apenergy.2020.114566
- Cheng, T., Kang, H., Du, X., Li, Q., Bai, B., and Jia, H. (2017). Non-marine sequence stratigraphic characteristics of Nanjing Formation, northern Songlike basin. *Fault-Block Oil Gas Field* 24 (4), 481–485.
- Ding, F., Zhang, J., Xie, J., Li, C., Shi, C., Zhang, P., et al. (2014). Fine description of structure and sedimentary microfacies of Li32 block of Lijin oilfield, Dongying depression, China. *Arab. J. Geosci.* 7 (5), 1693–1704. doi:10.1007/s12517-013-0972-8
- Eyles, N., Eyle, s. C., and Miall, A. D. (2010). Lithofacies types and vertical profile models; an alternative approach to the description and environmental interpretation of glacial diamict and diamictite sequences. *Sedimentology* 33 (1), 151. doi:10.1111/j.1365-3091.1983.tb00679.x
- Feng, Z., and Zhang, S. (2012). Depositional evolution and accumulation response of Yautia-Nanjing Formation in Songlike basin. *Earth Sci. Front.* 19 (1), 78–87.
- Folk, R. (1968). *Petrology of sedimentary rocks*. Austin: Hemphill Publishing Company.
- Gao, Y., Qu, X., Jiang, L., Wang, S., and Wang, P. (2017). Lithology and stratigraphic interfaces prediction of the continental scientific drilling project of cretaceous Songlike basin. *Earth Sci. Front.* 24 (1), 242–256.
- Gao, Y., and Wang, P. (2010). Sedimentary facies and cyclostratigraphy of the Cretaceous first member of Nanjing Formation in the Southeast uplift zone, Songlike Basin and its correlation with the CCSD-SK-I. *Acta Petrol. Sin.* 26 (1), 99–108.
- Gugliotta, M., Flint, S., Hodgson, D., and Veiga, G. (2015). Stratigraphic record of river-dominated crevasse subdeltas with tidal influence (lajas formation, Argentina). *J. Sediment. Res.* 85 (3), 265–284. doi:10.2110/jsr.2015.19
- Guo, S., and Mao, W. (2019). Division of diagenesis and pore evolution of a permian shanxi shale in the ordos basin, China. *J. Petrol. Sci. Eng.* 182, 106351. doi:10.1016/j.petrol.2019.106351
- Huang, W., Zhang, S., Zhang, C., and Wei, W. (2013). Sequence configuration and sedimentary evolution of Nanjing formation in the Songlike Basin. *Acta Sedimentol. Sin.* 31 (5), 920–927.
- Jia, J., Wang, P., Shao, R., Cheng, R., Zhang, B., Hou, J., et al. (2007). Stratigraphical sequence and regional correlation of yingcheng Formation in the southeast of Songlike basin. *J. Jilin Univ.* 37 (6), 1110–1123.
- Jin, J., Liu, D., Ji, Y., Yang, Z., Gao, C., Wang, J., et al. (2019). Research on lithofacies types, cause mechanisms and distribution of a gravel braided-river alluvial fan: a case study of the modern Poplar river alluvial fan, northwestern Junggar Basin. *Acta Sedimentol. Sin.* 37 (2), 254–267.
- Kallepalli, A., and Richardson, M. (2017). Digital shoreline analysis system-based change detection along the highly eroding Krishna–Godavari delta front. *J. Appl. Remote Sens.* 11 (3), 36018–36011. doi:10.1117/1.JRS.11.036018
- Li, G., Wan, X., Batten, D., Bengtson, P., Xi, D., and Wang, P. (2009). Spinicaudatans from the upper cretaceous Nanjing Formation of the Songlike basin, northeast China: taxonomy and biostratigraphy. *Cretac. Res.* 30 (3), 687–698. doi:10.1016/j.cretres.2008.12.008
- Li, J., Liu, S., Zhang, J., Fan, Z., Sun, Z., Zhang, M., et al. (2015). Architecture and facies model in a non-marine to shallow-marine setting with continuous base-level rise: an example from the cretaceous Denglouku Formation in the Changling depression, Songlike Basin, China. *Mar. Petrol. Geol.* 68, 381–393. doi:10.1016/j.marpetgeo.2015.09.002
- Li, S., Li, H., Xu, W., and Dong, Z. (2007). Sequence architectures and sedimentary features of lower cretaceous in the southern Songlike Basin. *Nat. Gas. Ind.* 27 (4), 36–39.
- Li, X., Zhang, J., Liu, L., Fan, Z., and Meng, N. (2018). Reservoir architecture and fracture characterization of low-permeability sandstone reservoir: a case study of Biandong oilfield, Jinhu depression, northern Jiangsu Basin, China. *Arab. J. Geosci.* 11 (14), 380. doi:10.1007/s12517-018-3682-4
- Li, Y., Chang, X., Yin, W., and Wang, G. (2019). Quantitative identification of diagenetic facies and controls on reservoir quality for tight sandstones: a case study of the Triassic Chang 9 oil layer, Zhenjing area, Ordos Basin. *Mar. Petrol. Geol.* 102, 680–694. doi:10.1016/j.marpetgeo.2019.01.025
- Li, Z., Lu, S., Li, J., Xiao, D., Chen, H., and Li, Y. (2017). Sedimentary characteristics and evolution of member 1 of Yautia Formation of cretaceous in zhaoyuan-taipingchuan area of Songlike basin. *J. Petrol. Sci. Eng.* 148, 52–63. doi:10.1016/j.petrol.2016.09.038
- Liu, H., Miao, H., Chen, W., Li, L., and Bai, L. (2003). Resource potential in the shallow middle part of Songlike Basin. *China Pet. Explor.* 8 (3), 13–17.
- Liu, L., Zhang, J., Wang, R., Wang, J., Yu, J., Sun, Z., et al. (2016). Facies architectural analysis and three-dimensional modeling of Wen79 fault block, Wellie oilfield, Donghu depression, China. *Arab. J. Geosci.* 9 (18), 714. doi:10.1007/s12517-016-2749-3
- Liu, Z., Wang, D., Liu, L., Liu, W., Wang, P., Du, X., et al. (1993). Sedimentary characteristics of the cretaceous in the Songlike basin. *Acta Geologica Sin.* 6 (2), 167–180.
- Lv, Da., Wang, D., Li, Z., Liu, H., and Li, Y. (2016). Depositional environment, sequence stratigraphy and sedimentary mineralization mechanism in the coal bed- and oil shale-bearing succession: a case from the Paleogene Huangshan Basin of China. *J. Petrol. Sci. Eng.* 148, 32–51. doi:10.1016/j.PETROL.2016.09.028
- Meng, Q., Zhang, S., Sun, G., Fu, X., Wang, C., and Shang, Y. (2016). A seismic geomorphology study of the fluvial and lacustrine-delta facies of the Cretaceous Quantou-Nanjing Formations in Songlike Basin, China. *Mar. Petrol. Geol.* 78, 836–847. doi:10.1016/j.marpetgeo.2016.01.017
- Miall, A. (1985). Architectural-element analysis: a new method of facies analysis applied to fluvial deposits. *Earth Sci. Rev.* 22 (4), 261–308. doi:10.1016/0012-8252(85)90001-7
- Mo, W., Wu, C., Su, N., Zhang, S., and Wang, M. (2019). Seismic imaging of the sedimentary system of the upper 3 cretaceous Nanjing Formation in northern Songlike basin. *J. Earth Sci.* 30 (4), 1–11. doi:10.1007/s12583-017-0970-y
- Pan, S., Liu, H., Carlos, Z., Liu, C., Liang, S., Zhang, Q., et al. (2017). Sublacustrine hyperpycnal channel-fan system in a large depression basin: a case study of Nen 1 Member, Cretaceous Nanjing Formation in the Songlike Basin, NE China. *Petrol. Explor. Dev.* 44 (6), 911–922.
- Porten, K., Kane, I., Warcho, M., and Southern, S. (2016). A sedimentological process-based approach to depositional reservoir quality of deep-marine sandstones: an example from the springar formation, northwestern vring basin, Norwegian sea [J]. *J. Sediment. Res.* 86 (11), 1269–1286.
- Qi, Y., Zhang, Z., Zhou, M., and Zheng, W. (2009). Lithofacies and sedimentary facies from middle Triassic fluvial deposits of Youfangzhuang Formation, Jiyuan area, western Henan. *Acta Sedimentol. Sin.* 27 (2), 254–264.
- Shi, L., Jin, Z., Yan, W., Zhu, X., Xu, X., and Peng, B. (2015). Influences of overpressure on reservoir compaction and cementation: a case from northwestern subsag, Bozhong sag, Bohai Bay Basin, East China. *Petrol. Explor. Dev.* 42 (3), 339–347. doi:10.1016/S1876-3804(15)30024-0
- Sun, Y., Zhong, J., Jiang, Z., Yu, W., Cao, Y., and Rao, M. (2006). Study of sequence stratigraphy of depression period in southern Songlike Basin. *J. China Univ. Petrol.* 30 (5), 1–7.
- Tong, X., Hu, J., Xi, D., and Zhu, M. (2018). Depositional environment of the Late Santonian lacustrine source rocks in the Songlike Basin (NE China): implications from organic geochemical analyses. *Org. Geochem.* 124, 215–227.
- Wang, D.-d., Shao, L.-y., Li, Z.-x., Li, M.-p., Lv, D., and Liu, H. (2016). The hydrocarbon generation characteristics, reservoir performance and preservation conditions of continental coal measures shale gas. *J. Petrol. Sci. Eng.* 145, 609–628. doi:10.1016/j.petrol.2016.06.031
- Wang, J., Fu, J., Xie, J., and Wang, J. (2020). Quantitative characterisations of gas loss and numerical simulations of underground gas storage based on gas displacement experiments performed with systems of small-core devices connected in series. *J. Nat. Gas Sci. Eng.* 81, 103495. doi:10.1016/j.jngse.2020.103495
- Wang, J., Zhang, J., and Xie, J. (2018). Analysis of the factors that influence diagenesis in the terminal fan reservoir of fuyu oil layer in the southern Songlike basin, northeast China. *Open Geosci.* 10 (1), 866–881. doi:10.1515/geo-2018-0068
- Wang, J., Zhang, J., and Xie, J. (2014). Initial gas full-component simulation experiment of Ban-876 underground gas storage. *J. Nat. Gas Sci. Eng.* 18, 131–136. doi:10.1016/j.jngse.2014.02.006

- Wang, L., Wu, C., Mo, W., and Zhang, S. (2014). Sedimentary characteristics and identification of muddy deltaic in Nanjing Formation of Songlike basin. *Acta Sci. Naturalium Univ. Pekin.* 50 (3), 497–506.
- Wang, W., Min, W., Lu, S., Chen, S., Zheng, M., and Wu, X. (2016). Basin modelling of gas migration and accumulation in volcanic reservoirs in the Xujiaweizi fault-depression, Songlike Basin. *Arabian J. Geosci.* 9 (2), 166. doi:10.1007/s12517-015-2072-4
- Wu, D., Li, H., Jiang, L., Hu, S., Wang, Y., Zhang, Y., et al. (2019). Diagenesis and reservoir quality in tight gas bearing sandstones of a tidally influenced fan delta deposit: the Oligocene Zhuhai Formation, western Pearl River Mouth Basin, South China Sea. *Mar. Petrol. Geol.* 107, 278–300. doi:10.1016/j.marpetgeo.2019.05.028
- Wu, J., Liang, C., Hu, Z., Yang, R., Xie, J., Wang, R., et al. (2019). Sedimentation mechanisms and enrichment of organic matter in the ordovician wufeng formation-silurian longmaxi Formation in the sichuan basin. *Mar. Petrol. Geol.* 101, 556–565. doi:10.1016/j.marpetgeo.2018.11.025
- Xu, G., Liu, J., Gugliotta, M., Saito, Y., Chen, L., Zhang, X., et al. (2020). Link between East Asian summer monsoon and sedimentation in river-mouth sandbars since the early Holocene preserved in the Yangtze River subaqueous delta front. *Quat. Res.* 95, 84–96. doi:10.1017/qua.2020.1
- Xu, J., Liu, Z., Bechtel, A., and Sachsenhofer, R. (2019). Organic matter accumulation in the upper cretaceous Qingshankou and Nanjing formations, Songlike basin (NE China): implications from high-resolution geochemical analysis. *Mar. Petrol. Geol.* 102, 187–201.
- Yang, Y., Qiu, L., Cao, Y., and Cheng, C. (2017). Reservoir quality and diagenesis of the permian lucaogou formation tight carbonates in jimsar sag, junggar basin, west China. *J. Earth Sci.* 28 (6), 1032–1046. doi:10.1007/s12583-016-0931-6
- Ye, D. (2005). Lower cretaceous sequence stratigraphic framework and hydrocarbon accumulation in the southeast rise, Songlike Basin, China. *Chin. J. Geol.* 40 (2), 227–236.
- Zhang, C., Zhang, S., Wei, W., Wu, C., Liang, J., Niu, W., et al. (2014). Sedimentary filling and sequence structure dominated by T-R cycles of the Nanjing Formation in the Songlike Basin. *Sci. China Earth Sci.* 57 (2), 278–296.
- Zhang, M., and Wang, Y. (2019). Paleoseismic event recorded in the upper cretaceous Nanjing Formation in southeastern area of the Songlike basin (NE China). *Aust. J. Earth Sci.* 66 (1), 95–110. doi:10.1080/08120099.2018.1499550
- Zhang, P., Zhang, J., Wang, J., Li, M., Liang, J., and Wang, Y. (2018). Flow units classification for geostatistical three-dimensional modeling of a non-marine sandstone reservoir: a case study from the Paleocene funing formation of the Gaoji oilfield, East China. *Open Geosci.* 10 (1), 113–120. doi:10.1515/geo-2018-0009
- Zhang, X., and Huang, Y. (2010). Sedimentary evolution characteristics of the Nanjing formation in the southern Songlike Basin. *J. Yangtze Univ.* 7 (1), 165–167.
- Zhang, X., Pang, X., Jin, Z., et al. (2020). Depositional model for mixed carbonate-clastic sediments in the middle cambrian lower zhangxia formation, xiaweidian, north China. *Adv. Geo-Energy Res.* 4 (1), 29–42. doi:10.26804/ager.2020.01.04

Conflict of Interest: The authors declare that the research was conducted in the absence of any commercial or financial relationships that could be construed as a potential conflict of interest.

The reviewer DL declared a past coauthorship with one of the authors, JW, and the handling editor. The reviewer CL declared a past coauthorship with one other author, JX, and the handling editor.

Copyright © 2021 Wang, Fu, Wang, Zhao, Zhang and Liu. This is an open-access article distributed under the terms of the Creative Commons Attribution License (CC BY). The use, distribution or reproduction in other forums is permitted, provided the original author(s) and the copyright owner(s) are credited and that the original publication in this journal is cited, in accordance with accepted academic practice. No use, distribution or reproduction is permitted which does not comply with these terms.